J. Biochem. 2012;152(3):221–229 doi:10.1093/jb/mvs061

JB THE JOURNAL OF BIOCHEMISTRY

C–H . . . π interplay between Ile308 and Tyr310 residues in the third repeat of microtubule binding domain is indispensable for self-assembly of three- and four-repeat tau

Received February 14, 2012; accepted May 1, 2012; published online June 1, 2012

Koushirou Sogawa[1,*], Ryouhei Okuda[1,*], Yasuko In[1], Toshimasa Ishida[1], Taizo Taniguchi[2], Katsuhiko Minoura[1,†] and Koji Tomoo[1,‡]

[1]Department of Physical Chemistry, Osaka University of Pharmaceutical Sciences, 4-20-1 Nasahara, Takatsuki, Osaka 569-11 and [2]Department of Pharmaceutical Health Care, Faculty of Pharmaceutical Sciences, Himeji Dokkyo University, 7-2-1 Kamiohno, Himeji, Hyogo 670-8524, Japan

[†]Katsuhiko Minoura, Research Center, Osaka University of Pharmaceutical Sciences, 4-20-1 Nasahara, Takatsuki, Osaka 569-1094, Japan. Fax: +81 726 90 1039, Tel: +81 726 90 1068, e-mail: minoura@gly.oups.ac.jp.

[‡]Koji Tomoo, Department of Physical Chemistry, Osaka University of Pharmaceutical Sciences, 4-20-1 Nasahara, Takatsuki, Osaka 569-1094, Japan. Fax/Tel: +81 726 90 1068. e-mail: tomoo@gly.oups.ac.jp.

*These authors contributed equally to this work.

Information on the structural scaffold for tau aggregation is important in developing a method of preventing Alzheimer's disease (AD). Tau contains a microtubule binding domain (MBD) consisting of three or four repeats of 31 and 32 similar residues in its C-terminal half. Although the key event in tau aggregation has been considered to be the formation of β-sheet structures from a short hexapeptide ^{306}VQIVYK^{311} in the third repeat of MBD, its aggregation pathway to filament formation differs between the three- and four-repeated MBDs, owing to the intermolecular and intramolecular disulphide bond formations, respectively. Therefore, the elucidation of a common structural element necessary for the self-assembly of three-/four-repeated full-length tau is an important research subject. Expanding the previous results on the aggregation mechanism of MBD, in this paper, we report that the C–H . . . π interaction between the Ile308 and Tyr310 side chains in the third repeat of MBD is indispensable for the self-assembly of three-/four-repeated full-length tau, where the interaction provides a conformational seed for triggering the molecular association. On the basis of the aggregation behaviours of a series of MBD and full-length tau mutants, a possible self-association model of tau is proposed and the relationship between the aggregation form (filament or granule) and the association pathway is discussed.

Keywords: C–H . . . π interaction/isoleucine residue/microtubule binding domain/tau protein/tyrosine residue.

Abbreviations: AD, Alzheimer's disease; CD, circular dichroism; DTT, dithiothreitol; EM, electron microscopy; His, histidine; MBD, microtubule binding domain; MT, microtubule; PHF, paired helical filament; ThS, thioflavin S; 3Rtau, three repeat full-length tau; 4Rtau, four repeat full-length tau; 3RMBD, three-repeated MBD; 4RMBD, four-repeated MBD.

Tau is a major microtubule (MT)-associated protein that is also the main component of the aberrant filaments like the neuropil threads or the neurofibrillary tangles (*1*, *2*), found in the brain of Alzheimer's disease (AD) patients. Tau is highly soluble and adopts a natively unfolded structure in solution. However, in the brains of AD patients, tau dissociates from axonal MTs through extensive phosphorylation and aggregates to form an insoluble paired helical filament (PHF) called the neurofibrillary tangle (*3*–*9*). Information on the mechanism of PHF formation of tau is important for elucidating the mechanisms and the development of therapeutic drugs for AD.

In the central nervous system of the adult human brain, six tau isoforms are expressed ranging in size from 352 to 441 amino acids (Fig. 1) (*10*–*12*). Tau contains a microtubule binding domain (MBD) consisting of three or four repeats of 31 and 32 similar amino acid sequences in the C-terminal half, and binds to and stabilizes microtubules (*13*–*15*). Generally, the key event in tau polymerization is the formation of a β-strand structure from the short hexapeptide ^{306}VQIVYK^{311} in the third repeat of MBD (*16*, *17*), where the residual number corresponds to the longest isoform. An X-ray crystal analysis of this peptide showed that it adopts a β-strand conformation and forms β-sheets with neighbouring peptides that combine in a face-to-face interdigitating 'steric zipper' structure (*18*).

Tauopathies can be characterized on the basis of the isoform composition of their filaments (*19*, *20*). For example, filaments in Pick disease contain three repeats (3R: R1-R3-R4), whereas those in progressive supranuclear palsy and corticobasal degeneration contain four repeats (4R: R1–R2–R3–R4). Filaments in AD incorporate three- and four-repeated tau. On the other hand, we previously reported that the association pathway of four-repeated MBD (4RMBD) is different from that of three-repeated MBD (3RMBD) in the

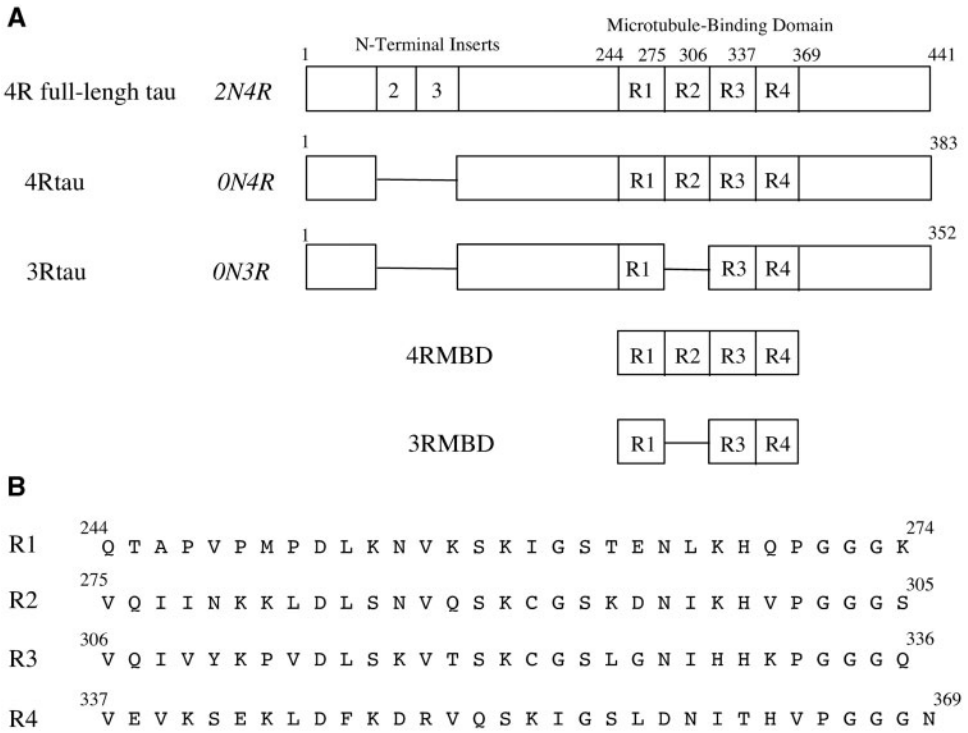

Fig. 1 Schematic representations of (**A**) longest 4R-tau isoform including two N-terminal inserts (*2N4R*) among six different tau isomers, together with three- and four-repeat isomers of 4Rtau (*0N4R*), 3Rtau (*0N3R*), 4RMBD and 3RMBD used in this work and (**B**) amino acid sequences of first to fourth repeats (R1–R4). Residual numbering is adapted to that of the longest isoform 4Rtau (441 residues).

following points: (i) the elemental unit for the association is an intermolecular Cys–Cys disulphide-bonded dimer between the neighbouring third repeats (R3) for 3RMBD and an intramolecular disulphide-bonded monomer between the second (R2) and third (R3) repeats for 4RMBD (*21*, *22*), and (ii) the presence of dithiothreitol (DTT), a reducing agent, decreases the filament formation ability of 3RMBD, but it increases that of 4RMBD (*23*). Therefore, information on the common structural element that enables the initial self-association of three- and four-repeated MBD (3R/4RMBD) or tau (3R/4Rtau) is crucial for developing AD inhibitors. Recently, we reported the importance of Tyr located at position 310 (*24*) and of its interplay with Ile308 in the progress of the filament formation of 4RMBD (*25*). Thus, it is important upon confirming the universal role of this interplay in the initial association to examine whether the interplay between these Ile and Tyr residues is similarly indispensable for the filament formation of 3RMBD and 3R/4Rtau. In this article, we report that the interplay of Ile308 and Tyr310 residues is the least indispensable structural element for initiating the molecular association of 3R/4Rtau as well as of 3R/4RMBD, and the C–H$\ldots\pi$ interaction formed between their side chains functions as a conformational seed for triggering molecular self-association. Although the mechanism of tau PHF formation is not yet completely elucidated, the present result provides important information on key residues and structural scaffolds essential for initiating the molecular association, which is useful for designing AD inhibitors.

Experimental procedures

Chemicals

General laboratory chemicals and molecular biology reagents [heparin with a mean molecular weight around 6,000, and thioflavin S (ThS)] were purchased from (Sigma Co, MO, U.S.A.).

Preparation of VQIVYK residue-substituted MBD and tau mutants

A cDNA (clone T9) encoding the human brain tau gene (*2N4R*, *0N4R* and *0N3R*) was provided by Professor H. Mori (Osaka City University). Wild-type four repeat full-length tau (4Rtau), three repeat full-length tau (3Rtau) 4RMBD, and 3RMBD constructs (Fig. 1) were prepared by polymerase chain reaction amplification, using clone T9 as the template, as previously reported (*24*). The gene expression in *Escherichia coli* and the purification of histidine (His)-tagged 4R/3RMBD and 4R/3Rtau were performed as described in a previous article (*21*), and the purity of the recombinant protein was confirmed on the basis of a single band by SDS–PAGE.

A series of VQIVYK residue-substituted genes or Cys-substituted genes of His-tagged 4R/3RMBD and 4Rtau/3Rtau were obtained using several wild-type tau DNA, mutagenized primers and the QuikChange site-directed mutagenesis kit from (Stratagene, CA, U.S.A.). The gene expression and purification of a His-tagged mutant were performed in the same manner as that of the wild protein. The purity of each mutant was confirmed on the basis of a single band by SDS–PAGE. The sample concentration was determined by Bradford protein assay, measuring 280 nm UV absorption ($\varepsilon = 1280\,\mathrm{mol^{-1}\,l\,cm^{-1}}$ for Tyr residue).

ThS fluorescence measurement

A solution of each sample at 25 μM were prepared using 50 mM Tris–HCl buffer (pH 7.6), and 10 μM ThS was added. After adding 6.25 μM heparin, fluorescence intensity was measured with a JASCO FP-6500 instrument at 25°C, with an excitation at 440 nm and an emission at 500 nm. The background fluorescence of each sample solution was subtracted when needed. The averaged value of three times measurements was used for the data presentation.

Circular dichroism measurement

A solution of each sample at 25 μM were prepared using 20-mM phosphate buffer (pH 7.6). After adding 6.25 μM heparin, the circular dichroism (CD) spectral change was measured with a JASCO J-820 spectrometer at 25°C. For each experiment, eight spectra were summed up, and the molar ellipticity was determined after normalizing for the protein concentrations.

Electron microscopy measurement

A solution of each sample at 25 μM was mixed with 6.25 μM heparin in 50 mM Tris–HCl buffer (pH 7.6) and then incubated at 37°C for 48 h. Sample solutions (10 μl) were placed on 600-mesh copper grids and negatively strained with 2% uranyl acetate for 1 min. The specimens were examined with an electron microscope (Hitachi Co., Tokyo, Japan) operated at 75 kV.

Results

Interplay between Ile and Tyr residues in the R3 repeat is essential for the aggregation of 3RMBD as well as of 4RMBD

The aggregation behaviours of a series of 3RMBD mutants, in which the residue of the ^{306}VQIVYK^{311} sequence was substituted with Ala or Tyr, were investigated by ThS fluorescence measurement, CD spectroscopy and EM. The results are summarized in Table I, in which some results of 4RMBD mutants (*25*) are given for comparison. Selected examples are shown in Fig. 2. The ThS fluorescence intensity of the monosubstituted mutant by Ala showed that the mutation of I308 or Y310 residue causes the complete disappearance of the filament formation, although the Ala mutation of other residues still has aggregation ability with a detectable extent (data not shown). To investigate the importance of Tyr at position 310 in the aggregation of 3RMBD, the aggregation behaviours of a series of Y310A-fixed and Tyr-scanned mutants of the ^{306}VQIVYK^{311} sequence were investigated. Consequently, the following two important results were observed. First, the aggregation ability of 3RMBD is considerably lost only by Y310A regardless of the Tyr substitution for other residues in the ^{306}VQIVYK^{311} sequence, except Q307Y/Y310A. These mutants inhibited filament formation, although a small number of granulated aggregates were formed. In particular, the complete loss of aggregates was induced by I308Y/Y310A. Such a remarkable loss of aggregation ability by Y310A was also observed for 4RMBD, indicating that Tyr310 in the third repeat of MBD is essential for the filament formation despite the number of repeats. Second, Q307Y/Y310A shows a high aggregation ability and has a similar filament morphology to 3RMBD. This suggests that the self-association mechanism of Q307Y/Y310A is essentially the same as that of 3RMBD (discussed later).

The complete loss of the aggregation abilities of I308A, Y310A and I308Y/Y310A indicates clearly that the interplay between I308 and Y310 residues is essential for the molecular aggregation of 3RMBD. It is clear from Table I that these aggregation behaviours are almost the same as those of 4RMBD. Previously, we reported that the building units for molecular aggregation are different between 3RMBD and 4RMBD (*22*), that is, the intermolecular R3–R3 disulphide-bonded dimer for 3RMBD and the intramolecular R2–R3 disulphide-bonded monomer for 4RMBD. However, the present result indicates that the interplay between I308 and Y310 residues in the R3 repeat is a common structural element indispensable for initiating the molecular association of both MBDs.

Interplay between I308 and Y310 residues is based on the C–H . . . π interaction

The comparison between the aggregation abilities of wild MBD and its I308A or Y310A mutant (Table I)

Table I. Comparison of ThS fluorescences, CD amplitudes and EM morphologies of 3RMBD/4RMBD and their mutants (25 μM)[a,b].

	Without DTT			With DTT	
Wild/Mutant	Relative fluorescence intensity (%)	Relative change (%) of molar ellipticity at 200 nm	EM morphology	Relative fluorescence intensity (%)	EM morphology
3RMBD	100	100	Filament	25	Short filament
Y310A	0	0	No granule and no filament	0	No granule and no filament
I308A	0	0	No granule and no filament	0	No granule and no filament
I308V	60	50	Short filament	20	Short filament
I308Y/Y310A	0	0	No granule and no filament	0	No granule and no filament
I308Y/Y310I	0	0	No granule and no filament	0	No granule and no filament
Q307Y	250	150	Filament + granule(+2)	300	Granule(+2)
Q307Y/Y310A	70	40	Short filament	20	Short filament
Q307Y/V309A/Y310A	0	0	No granule and no filament	0	No granule and no filament
4RMBD	100	100	Filament	120	Filament
Y310A	0	0	No granule and no filament	0	No granule and no filament
I308A	0	0	No granule and no filament	0	No granule and no filament
I308V	90	90	Filament	120	filament
I308Y/Y310I	0	0	No granule and no filament	0	No granule and no filament
Q307Y	300	150	Filament + granule(+2)	300	Filament + granule(+2)
Q307Y/Y310A	100	90	Filament	120	Filament
Q307Y/V309A/Y310A	0	0	No granule and no filament	0	No granule and no filament

[a]The fluorescence intensities and CD amplitudes of mutants correspond to values relative to those of wild 3RMBD and 4RMBD without DTT at 1 h after initiating aggregation by addtion of heparin.
[b]EM morphology at 48 h after initiating aggregation by addition of heparin.

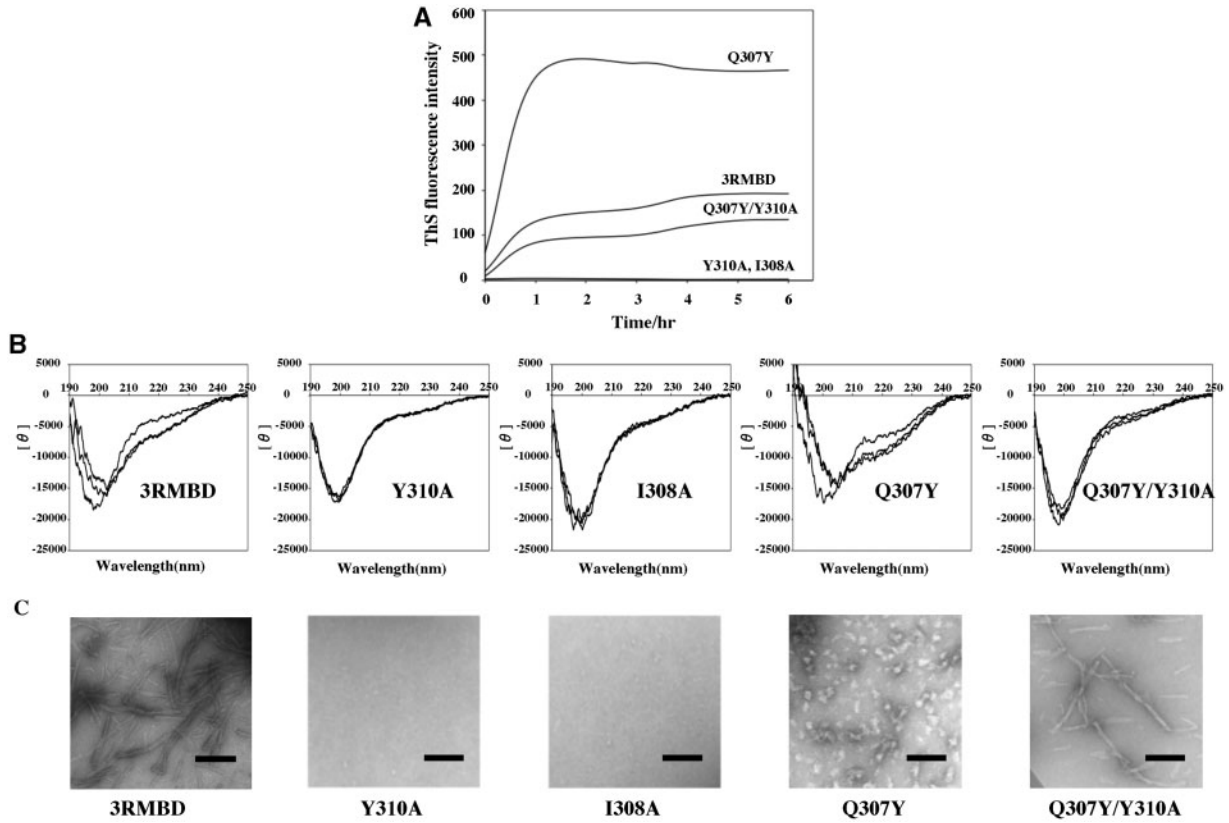

Fig. 2 (**A**) Time-dependent ThS fluorescence intensity profiles, (**B**) time-dependent CD spectral changes and (**C**) negative-staining EM images of 3RMBD and its Y310A, I308A, Q307Y and Q307Y/Y310A mutants. The Q307Y/V309A/Y310A mutant shows essentially the same results as I308A. The respective CD spectra from bottom to top at the 200 nm correspond to those obtained at 0 min, 3, 6 and 24 h after adding heparin to the solution. The length of the bar in (C) corresponds to 500 nm.

indicates that the interplay between I308 and Y310 is based on the C–H . . . π interaction between their residues, where the C–H group of the Ile side chain interacts with the π electron of the Tyr phenyl ring. This is supported by the suppressed aggregation ability of I308V compared with that of the wild type because Val has a lower hydrophobicity than Ile. It is important to note that the filament formation *via* the C–H . . . π interaction is dependent on the positional relationship between Ile and Tyr residues because I308Y/Y310I showed a complete loss of their molecular aggregation ability, similarly to the case of I308Y/Y301A. This clearly indicates that Ile should be located on the N-terminal side compared with Tyr, that is, the C–H . . . π interaction should be formed along the N side → C side direction of the sequence.

As could be deduced from the aggregation behaviours of the Q307Y, Q307Y/Y310A and Q307Y/V309A/Y310A of 3R/4RMBD, a structural requirement for filament formation *via* the C–H . . . π interaction is a planar backbone of the ^{306}VQIVYK^{311} sequence. The ^{306}VQIVYK^{311} sequence in the R3 repeat was previously showed to be planar by NMR analysis in both aqueous and 2,2,2-trifluoroethanol solutions (*26*) and X-ray crystal structure (*18*). The planar conformation of ^{306}VYIVYK^{311} sequence in the Q307Y enables an intramolecular C–H . . . π interaction between I308 and Y310 residues on one side of

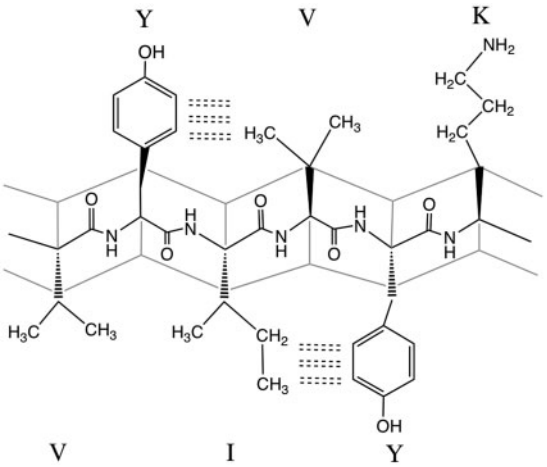

Fig. 3 Double C–H . . . π interactions of Q307Y–V309 and I308–Y310 pairs on both sides of planar VYIVYK backbone of R3 repeat in Q307Y mutant.

the plane and a similar C–H . . . π interaction between the Y307 and V309 residues on the opposite side (Fig. 3). These C–H . . . π interactions on both sides could almost be related with a 2-fold symmetry running along the centre of a pleated peptide plane of the VYIVYK sequence. This would be the reason Q307Y markedly increased aggregation rate, which became 3-fold higher than that of wild MBD. The similar

aggregation ability of Q307Y/Y310A to that of wild MBD and the complete lack of the aggregation ability of Q307Y/V309A/Y310A also support the C–H . . . π interaction between the V309 and Y307 side chains.

C–H . . . π interaction between Ile and Tyr residues in R3 repeat is essential for the molecular aggregation of 3R/4Rtau

To determine whether the common structural element indispensable for starting the molecular association of 3R/4RMBD is also applicable to that of full-length tau, a series of ^{306}VQIVYK^{311} residue-substituted mutants of 3R/4Rtau were prepared and examined for their aggregation behaviours. The results are given in Table II, and some examples are shown in Fig. 4.

The CD spectra of 3R/4Rtau and their mutants showed no notable conformational change for >6 h after starting aggregation. This may result from that the flexible sequences bound to both sides of MBD affect the aggregation behaviour of tau in such a way that the structural change accompanied by the MBD aggregation is not smoothly propagated toward the whole structure. However, it is clear that the C–H . . . π interaction between I308 and Y310 residues is indispensable to the filament formation of 3R/4Rtau. The I308A and Y310A of 3R/4Rtau completely lost their aggregation ability. In contrast, I308V or Y310W showed similar aggregation ability to 4Rtau. A marked increase in the aggregation rate of Q307Y, probably due to double C–H . . . π interactions of Y307–V309 and I308–Y310 pairs, was also observed for 3R/4Rtau. These results clearly confirm the importance of the C–H . . . π interaction between the I308 and Y310 residues for the filament formation of tau as well as of its MBD.

On the other hand, the difference between the aggregation behaviours of tau and MBD was observed in the ThS fluorescence intensity and electron microscopy (EM) morphology of their Q307Y/Y310A mutants. The Q307Y/Y310A of 3R/4Rtau no longer showed notable aggregation behaviour such as that of 3R/4RMBD, indicating that the single C–H . . . π interaction from the back side on the planar hexapeptide in the R3 repeat is not passable for the molecular aggregation of tau. This would be due to the effect of the N- and C-terminal flexible regions bound to both sides of MBD, because the N- and C-terminal regions remain largely disordered, form a fuzzy coat and fold back onto the repeats (*27*) to form transient intramolecular contact (*28*). In such a situation, it would be reasonable to consider that the filament formation of 3R/4Rtau proceeds via the C–H . . . π interaction between Ile308 and Tyr310 residues on one side of the R3 repeat, although no such a structural restriction is required up to the granule formation stage, as observed for Q307Y.

Different effect of reducing agent on molecular aggregations of MBD and tau

Our previous study clarified that the building units for 3RMBD and 4RMBD are intermolecular R3–R3 disulphide-bonded dimers and intramolecular R2–R3 disulphide-bonded monomers, respectively (*22*), and this difference results in the marked suppression and enhancement of the molecular aggregations of 3RMBD and 4RMBD, respectively, by the addition of DTT, a reducing agent (*23*). To confirm the effect of DTT on the molecular aggregations of 3R/4Rtau, the aggregation behaviours of the respective wild-type and mutants with and without DTT were compared in terms of the ThS fluorescence intensity and EM morphology; the results are given in Table II.

As previously reported, DTT enhanced the molecular aggregation of both wild and mutant 4RMBDs including a single C–H . . . π interaction, whereas the molecular aggregations of 3RMBD and its mutant via a single C–H . . . π interaction were considerably suppressed by DTT. DTT increased the fluorescence

Table II. Comparison of ThS fluorescences and EM morphologies of 3Rtau/4Rtau and their mutants (25 μM)[a,b].

	Without DTT		With DTT	
Wild/Mutant	Relative fluorescence intensity (%)	EM morphology	Relative fluorescence intensity (%)	EM morphology
3Rtau	100	Filament	10	Granule(+1)
I308A	0	No granule and no filament	0	No granule and no filament
Y310A	0	No granule and no filament	0	No granule and no filament
Q307Y	300	Granule(+2)	300	Granule
Q307Y/Y310A	10	Granule(+1)	0	No granule and no filament
4Rtau	100	Filament	10	Glanule(+1)
I308A	0	No granule and no filament	0	No granule and no filament
I308V	40	Short filament	5	No granule and no filament
Y310A	0	No granule and no filament	0	No granule and no filament
Y310W	100	Filament	150	Filament
I308Y/Y310I	0	No granule and no filament	0	No granule and no filament
Q307Y	300	Granule(+2)	300	Granule(+2)
Q307Y/Y310A	10	No granule and no filament	5	No granule and no filament
Q307Y/V309A/Y310A	0	No granule and no filament	0	No granule and no filament

[a]The fluorescence intensities of mutants correspond to the values relative to those of wild 3Rtau and 4Rtau without DTT at 1 h after initiating aggregation by addition of heparin.
[b]EM morphology at 48 h after initiating aggregation by addition of heparin.

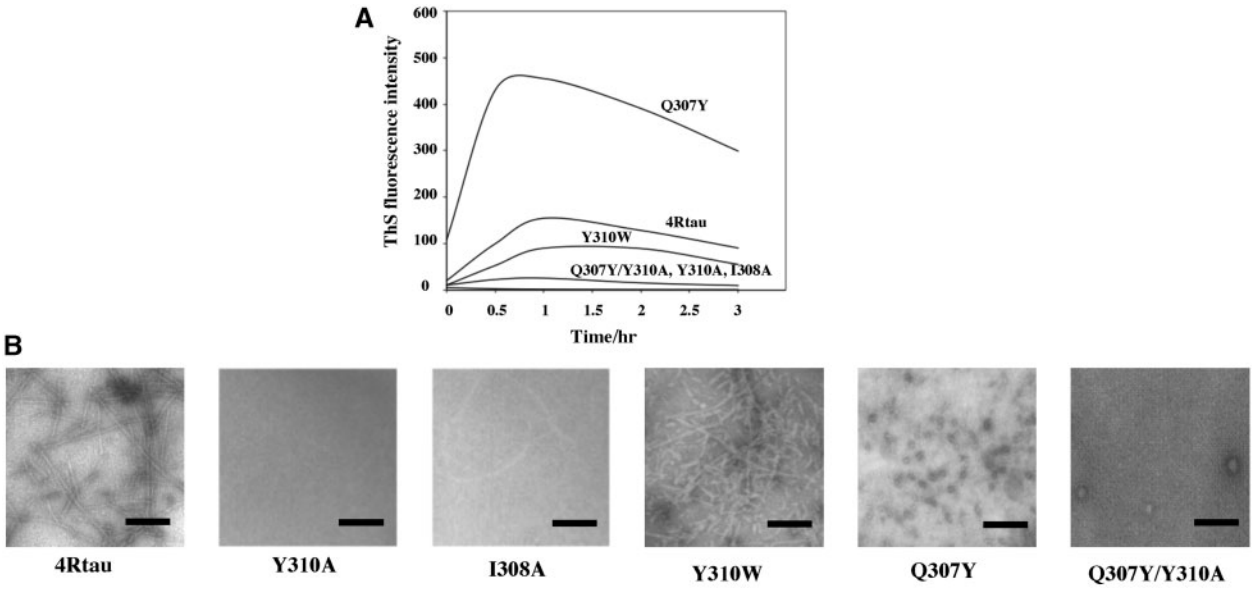

Fig. 4 (**A**) Time-dependent ThS fluorescence intensity profiles and (**B**) negative-staining EM images of 4Rtau and its Y310A, I308A, Y310W, Q307Y and Q307Y/Y310A mutants. The Q307Y/V309A/Y310A mutant shows essentially the same results as those of I308A. The length of the bar in (B) corresponds to 500 nm.

intensity of 4RMBD to nearly the same extent as that of 3RMBD without DTT, and this would indicate that the folded structure of the intramolecular R2–R3 disulphide-bonded 4RMBD is disadvantageous for the aggregation and the DTT-induced open structure confers 4RMBD similar aggregation ability to that of 3RMBD dimers, because we clarified that 4RMBD under a reduced solution is composed of the intermolecular associated dimers (*21*). In contrast, the DTT-induced transition of the intermolecular R3–R3 disulphide-bonded dimer of 3RMBD to the monomer lost its original aggregation ability.

On the other hand, the 3R/4Rtau showed a different behaviour from 3R/4RMBD. The ThS intensities of 3R/4Rtau were both decreased by the DTT addition, and this is in contrast to the cases of 3RMBD and 4RMBD, in which the DTT-dependent molecular aggregation process is dependent on, respectively, intermolecular and intramolecular disulphide bond formation. This discrepancy would mean that such disulphide bond formation is insufficient to control the overall aggregation behaviour of 3R/4Rtau, probably owing to the presence of flexible sequences attached to both the N- and C-terminal sides of MBD. However, the aggregation ability of the Q307Y mutant of 3R/4Rtau, as well as of 3R/4RMBD, having double C–H...π interactions within the R3 repeat was hardly affected by the addition of DTT. This would mean that the double C–H...π interactions on the R3 core moiety precede the disulphide bond formation for the molecular association, and the interaction provides the platform that is indispensable for starting molecular association, although it does not proceed to the mature filament formation.

To investigate the roles of the Cys291 and Cys322 residues of tau in the filament formation, Ala-substituted mutants of 4R/3RMBD and 3R/4Rtau were prepared. Their ThS fluorescence intensities and EM morphologies are given in Table III. The results showed the different role between the Cys residues of 3RMBD and 4RMBD in their filament formations; the results were about in accord with those of DTT effect on the intra/intermolecular disulphide bond formation in their molecular aggregations. In contrast, no notable difference was observed for 3R/4Rtau and these Ala-substituted mutants similarly decreased the ThS fluorescence intensities and transformed the filamentous morphology to small granules, similar to the case of DTT addition to wild 3R/4Rtau. This clearly indicates the participation of Cys residues in the second and third repeats in mature filament formation of tau. Therefore, we could state that intermolecular/intramolecular disulphide-bonded formation formed in 3R/4RMBD participates importantly in the filament

Table III. Comparison of ThS fluorescences and EM morphologies of C291A and/or C322A mutants of 4R/3RMBD and 4R/3Rtau (25 μM)[a,b].

Wild/Mutant	Relative fluorescence intensity (%)	EM morpohology
4RMBD	100	Filament
C291A	100	Filament
C322A	80	Filament
C291A/C322A	120	Filament
3RMBD	100	Filament
C322A	20	Short filament
4Rtau	100	Filament
C291A/C322A	20	Granule(+1)
3Rtau	100	Filament
C322A	10	Granule(+1)

[a]The fluorescence intensities of mutants correspond to values relative to those of wild-types at 1 h after initiating aggregation by addition of heparin.
[b]EM morphology at 48 h after initiating aggregation by addition of heparin.

formation of 3R/4Rtau, although DTT-dependent aggregation behaviour is different between MBD and tau.

Discussion

The filament formation of tau protein is based on short hexapeptide motif (VQIVYK) in the R3 repeat domain of MBD. This short motif has a planar conformation even though tau protein has a random structure. The VQIVYK sequence, in addition to its structural character, has a partially hydrophobic character and tend to make a cross β-structure, which is the core of PHF.

The crystal structure of the VQIVYK peptide reported by Sawaya *et al.* (*18*) provides a molecular view of the structural organization of the spine of tau fibrils. In the crystal structure, the peptide adopts a planar conformation and forms an anti-parallel β-sheet with a neighbouring peptide that combines in a face-to-face interdigitating dry 'steric zipper' structure, where the back surface of this β-sheet constitutes a wet interface linked through water molecules.

The planar backbone conformation of VQIVYK peptide enables the direct interactions between the Ile and Tyr side chains on the same side of the peptide plane and between the Gln and Lys side chains on the other side. Therefore, it would be reasonable in a polar environment such as an aqueous solution to consider that the C–H . . . π interaction between the side chains of the Ile and Tyr residues under the hydrophobic environment provides a conformational seed to form an anti-parallel β-sheet with the VQIVYK sequence of the other R3 repeat. As determined from the results given in Tables I and II, it could say that this C–H . . . π interaction is the common structural element for initiating the molecular association of 3R/4RMBD and 3R/4Rtau irrespective of their difference in aggregation pathway.

Generally, the filament formation of tau can be divided into the following stages: activation → nucleation → extension → PHF formation. The EM figures showed either a filament or a granule as the aggregation form of wild or mutant tau. Herein, we discuss the possible relation between the aggregation form (filament or granule) and its association stage. From the relationship between the dynamic light scattering (DLS) data and EM pictures, we previously reported that the granule forms of MBD correspond to the nucleation state, which does not further proceed to the extension stage, whereas the filament form proceeds to the stage of PHF formation (*23*). It is clear that wild 3R/4RMBD and 3R/4Rtau proceed to the PHF stage through continuous molecular piling irrespective of the number of repeats. Thus, as a possible reason why some mutants stop at the granular nucleation stage, it could say that such systematic piling is impossible because of the structural disorder probably due to an unsystematic molecular association, although the aggregation is allowed up to the nucleation stage to some extent. In the case of the Q307Y mutant, the double C–H . . . π interactions of Val309–Tyr307 and Ile308–Tyr310 pairs would enable the rapid aggregation progress up to the nucleation stage, but not up to the filament formation stage, and this would be further due to the disturbance of alternative hydrophobic/hydrophilic stacking layer of the molecules. The presence of N- and C-terminal flexible regions bound to both terminals of MBD affect the aggregation behaviour of full-length tau concerning the time dependence of CD spectral change and the effect of DTT on the aggregation, which are considerably different from those of MBD.

On the basis of previous results that the building units for molecular aggregations of 4RMBD and 3RMBD are intramolecular R2–R3 disulphide-bonded monomer and intermolecular R3–R3 disulphide-bonded dimer, respectively, possible aggregation pathway is proposed in Fig. 5A and B. The four-repeat tau forms an intramolecular Cys291–Cys322 disulphide bond between the second and third repeats under a physiological condition (Fig. 5A). This conformational restriction and the presence of Pro301 and Pro312 residues would enable the formation of a U-shaped structure at the R2–R3 linkage of 4RMBD, where these Pro residues are located at both corners. This model shows that the anti-parallely arranged MBDs pile up through the alternate hydrophobic and hydrophilic interactions among the neighbouring SVQIVYK β-strands along the fiber direction. In this model, the double C–H . . . π formation by the Q307Y mutation would change the hydrophilic interaction into the hydrophobic one, thus resulting in a rapid aggregation to the granule form in an aqueous solution. On the other hand, three-repeat tau would form a parallel dimer by the intermolecular disulphide bond of Cys322 residue in the third repeat (Fig. 5B). The parallel dimer would be stabilized by the hydrophilic interaction between the polar residues of SVQIVYK β-strands, where the VQIVYK plane in the Gly302–Lys311 sequence is rotatable around the ω torsion angles of Pro301–Gly302 and Lys311–Pro312 bonds because of the lack of a notable energy barrier between the *trans* and *cis* isomers at the Pro–Gly and Lys–Pro peptide bonds and of the lack of an intramolecular disulphide bond within MBD, different from the case of 4RMBD. The neighbouring parallel dimers would be stacked in an anti-parallel manner and piled up along the fiber direction through alternative hydrophobic/hydrophilic interactions among the KVQIVYK β-strands. The double C–H . . . π formation by Q307Y mutation would increase aggregation rate by the same reason as that for 4Rtau.

In conclusion, the present results indicated that two factors are important for molecular aggregation of tau: one is that the C–H . . . π interaction between Ile308 and Tyr310 side chains is an essential structural factor that enables the initial self-association of 3R/4Rtau as well as 3R/4RMBD and the other is that the intermolecular/intramolecular disulphide bond formation in 3R/4RMBD participates importantly in the filament formation of 3R/4Rtau. Although the mechanism of tau PHF formation remains to be elucidated, the present work provides important information on key residues and structural scaffolds essential for initiating the molecular association, which is important for designing AD inhibitors.

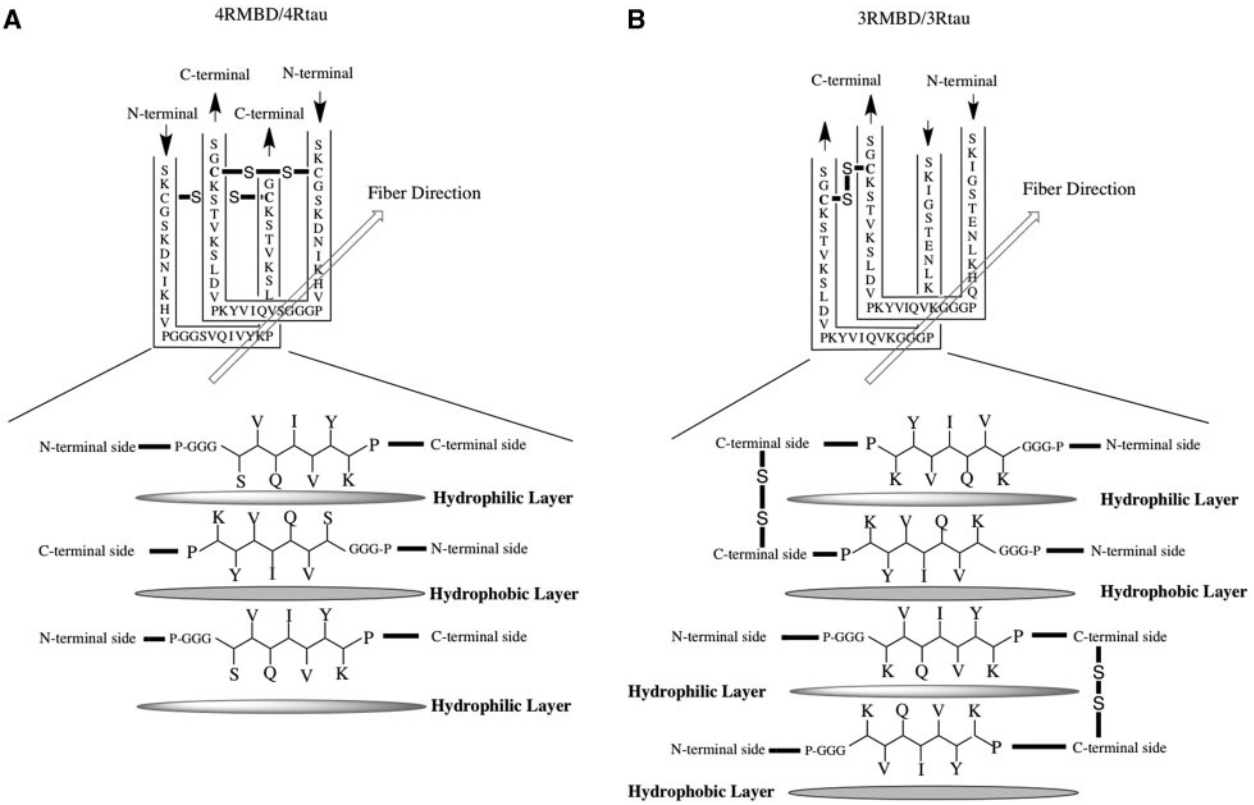

Fig. 5 Schematic aggregation models of (**A**) 4RMBD/4Rtau and (**B**) 3RMBD/3Rtau. The overall structure of 4R/3RMBD and its piling direction are shown on the upper side, and the alternate hydrophobic and hydrophilic interaction modes between neighbouring VQIVYK β-strands are shown on the lower side.

Funding
Grant-in-Aid for High Technology Research from the Ministry of Education, Culture, Sports, Science and Technology, Japan.

Conflict of interest
None declared.

References

1. Delacourte, A. and Buee, L. (1997) Normal and pathological tau proteins as factors for microtubule assembly. *Int. Rev. Cytol.* **171**, 167–224
2. Ballatore, C., Brunden, K.R., Trojanowski, J.Q., Lee, V.M.Y., Smith, A.B. III, and Huryn, D.M. (2011) Modulation of protein-protein interactions as a therapeutic strategy for the treatment of neurodegenerative tauopathies. *Curr. Top. Med. Chem.* **11**, 317–330
3. Goedert, M. and Spillantini, M.G. (2000) Tau mutations in frontotemporal dementia FTDP-17 and their relevance for Alzheimer's disease. *Biochim. Biophys. Acta.* **1502**, 110–121
4. Gendron, T.F. and Petrucelli, L. (2009) The role of tau in neurodegeneration. *Mol. Neurodegen.* **4**, 13
5. Braak, H. and Braak, E. (1991) Neuropathological staging of Alzheimer-related changes. *Acta. Neuro. Pathol.* **82**, 239–259
6. Bandyopadhyay, B., Li, G., Yin, H., and Kuret, J. (2007) Tau aggregation and toxicity in a cell culture model of tauopathy. *J. Biol. Chem.* **282**, 16454–16464
7. Maeda, S., Sahara, N., Saito, Y., Murayama, M., Yoshiike, Y., Kim, H., Miyasaka, T., Murayama, S., Ikai, A., and Takashima, A. (2007) Granular tau oligomers as intermediates of tau filaments. *Biochemistry* **46**, 3856–3861
8. Maeda, S., Sahara, N., Saito, Y., Murayama, S., Ikai, A., and Takashima, A. (2006) Increased levels of granular tau oligomers: an early sign of brain aging and Alzheimer's disease. *Neurosci. Res.* **54**, 197–201
9. Lasagna-Reeves, C.A., Castillo-Carranza, D.L., Guerrero-Munoz, M.J., Jackson, G.R., and Kayed, R. (2010) Preparation and characterization of neurotoxic tau oligomers. *Biochemistry* **49**, 10039–10041
10. Goedert, M., Spillantini, M.G., Portier, M.C., Ulrich, J., and Crowther, R.A. (1989) Cloning and sequencing of the cDNA encoding an isoform of microtubule-associated protein tau containing four tandem repeats: differential expression of tau protein mRNAs in human brain. *EMBO J.* **8**, 393–399
11. Goedert, M., Spillantini, M.G., Jakes, R., Rutherford, D., and Crowther, R.A. (1989) Multiple isoforms of human microtubule-associated protein tau: sequences and localization in neurofibrillary tangles of Alzheimer's disease. *Neuron* **3**, 519–526
12. Goedert, M. and Jakes, R. (1990) Expression of separate isoforms of human tau protein: correlation with the tau pattern in brain and effects on tubulin polymerization. *EMBO J.* **9**, 4225–4230
13. Lee, G., Neve, R.L., and Kosik, K.S. (1989) The microtubule-binding domain of tau protein. *Neuron* **2**, 1615–1624
14. Butner, K.A. and Kirschner, M.W. (1991) Tau protein binds to microtubules through a flexible array of distributed weak sites. *J. Cell. Biol.* **115**, 717–730

15. Goode, B.L. and Feinstein, S.C. (1994) Identification of a novel microtubule binding and assembly domain in the developmentally regulated inter-repeat region of tau. *J. Cell. Biol.* **124**, 769–782
16. Von Bergen, M., Friedhoff, P., Biernat, J., Heberle, J., Mandelkow, E.M., and Mandelkow, E. (2000) Assembly of tau protein into Alzheimer paired helical filaments depends on a local sequence motif ((306)VQIVYK(311)) forming beta structure. *Proc. Natl. Acad. Sci. USA* **97**, 5129–5134
17. Von Bergen, M., Barghorn, S., Li, L., Marx, A., Biernt, J., Mandelkow, E.M., and Mandelkow, E. (2001) Mutations of tau protein in front temporal dementia promote aggregation of paired helical filaments by enhancing local beta-structure. *J. Biol. Chem.* **276**, 48165–48174
18. Sawaya, M.R., Sambashivan, S., Nelson, R., Ivanova, M.I., Sievers, S.A., Apostol, M.I., Thompson, M.J., Balbirnie, M., Wiltzius, J.J.W., McFarlane, H.T., Madsen, A.O., Riekel, C., and Eisenberg, D. (2007) Atomic structures of amyloid cross-β spines reveal varied steric zipper. *Nature* **447**, 453–457
19. Hong, M., Zukareva, V., Vogelsberg-Ragaglia, V., Wszolek, Z., Reed, L., Miller, B., Geschwind, D.H., Bird, T.D., McKeel, D., Goate, A., Morris, J.C., Wilhelmsen, K.C., Schellenberg, G.D., Trojanowski, J.Q., and Lee, V.M.Y. (1998) Mutation-specific functional impairments in distinct tau isomers of hereditary FTDP-17. *Science* **282**, 1914–1917
20. Lu, M. and Kosik, K.S. (2001) Competition for microtubule-binding domain with dual expression of tau missense and splice isoforms. *Mol. Biol. Cell.* **12**, 171–184
21. Yao, T.M., Tomoo, K., Ishida, T., Hasegawa, H., Sasaki, M., and Taniguchi, T. (2003) Aggregation analysis of the microtubule-binding domain in tau protein by spectroscopic methods. *J. Biochem.* **134**, 91–99
22. Okuyama, K., Nishiura, C., Mizushima, F., Minoura, K., Sumida, M., Taniguchi, T., Tomoo, K., and Ishida, T. (2008) Linkage-dependent contribution of repeat peptides to self-aggregation of three- or four-repeat microtubule-binding domains in tau protein. *FEBS J.* **275**, 1529–1539
23. Sugino, E., Nishiura, C., Minoura, K., In, Y., Sumida, M., Taniguchi, T., Tomoo, K., and Ishida, T. (2009) Three-/four repeat-dependent aggregation profile of tau microtubule-binding domain clarified by dynamic light scattering analysis. *Biochem. Biophys. Res. Commun.* **385**, 236–240
24. Nishiura, C., Takeuchi, K., Minoura, K., Sumida, M., Taniguchi, T., Tomoo, K., and Ishida, T. (2010) Importance of Tyr310 residue in the third repeat of microtubule binding domain for filament formation of tau protein. *J. Biochem.* **147**, 405–414
25. Naruto, K., Minoura, K., Okuda, R., Taniguchi, T., In, Y., Ishida, T., and Tomoo, K. (2010) Interplay between I308 and Y310 residues in the third repeat of mucrotubule-binding domain is essential for tau filament formation. *FEBS Lett.* **584**, 4233–4236
26. Minoura, K., Tomoo, K., Ishida, T., Hasegawa, H., Sasaki, M., and Taniguchi, T. (2003) Solvent-dependent conformation of the third repeat fragment in the microtubule-binding domain of tau protein, analyzed by ^{1}H-NMR spectroscopy and molecular modeling calculation. *Bull. Chem. Soc. Jpn* **76**, 1617–1624
27. Jeganathan, S., Von Bergen, M., Brutlach, H., Steinhoff, H.J., and Mandelkow, E. (2006) Global hairpin folding of tau in solution. *Biochemistry* **45**, 2283–2293
28. Mukrasch, M.D., Bibow, S., Korukottu, J., Jeganathan, S., Biernat, J., Griesinger, C., Mandelkow, E., and Zweckstetter, M. (2009) Structural polymorphism of 441-residue tau at single residue resolution. *PLoS Biol.* **7**, e34